INVITED PAPER *Special Section on Heterogeneous Networks for Future Cellular Systems*

Comprehensive Analysis of Heterogeneous Networks with Pico Cells in LTE-Advanced Systems

Satoshi KONISHI[†a)], ***Member***

SUMMARY We have seen a rapid increase in mobile data traffic in cellular networks, especially in densely populated areas called "hotspots." In order to deal with this trend, heterogeneous networks (HetNet) are attracting much attention as a method of effectively accommodating such traffic increases using the Long Term Evolution (LTE)-Advanced system in the 3rd Generation Partnership Project (3GPP). This paper first presents an overview of HetNet, where various wireless nodes can be deployed over the coverage area formed by macro base stations (BSs). Next, various evaluation results are provided for HetNet, where pico BSs ("Pico-BSs") are deployed over the coverage area of macro BSs ("Macro-BSs"). Then, this paper presents a comprehensive analysis, not only of the effect of overlaying Pico-BSs but also a detailed analyses of the techniques called "cell range expansion (CRE)" and "enhanced inter-cell interference coordination (eICIC)" for facilitating the offloading of user terminals (UEs) from Macro-BSs to Pico-BSs and mitigating interference, respectively, for both downlink and uplink. Noteworthy outcomes found through the comprehensive study are that CRE provides throughput improvements for uplinks, especially for UE connected to Pico-BSs. In addition, this paper demonstrates that CRE contributes to improving downlink throughput especially for low traffic loads. The outcome regarding eICIC is that eICIC provides improvements in total throughput, in spite of the fact that eICIC causes unfairness between UE connected to the Pico-BSs and those with Macro-BSs.

key words: *heterogeneous networks, HetNet, pico base stations, CRE, eICIC*

1. Introduction

Mobile data traffic has recently been increasing rapidly along with the popularization of smartphones, with which we can enjoy video streaming services similar to using personal computers. According to the latest surveys, mobile data traffic in Japan more than doubled from 2010 to 2011 [1]. The International Telecommunication Union Radio Sector (ITU-R) summarized the trend in mobile data traffic and the future market trend for cellular systems in an ITU-R Report in October 2011 [2]. The ITU-R Report anticipates that mobile data traffic will increase tremendously in all countries and areas in the world, although the exact volume of the increase will vary by country and area.

In order to overcome such a surge in mobile data traffic, ITU-R standardized International Mobile Telecommunications Advanced (IMT-Advanced) systems in January 2012 [3]. In the ITU-R recommendation, Long Term Evolution Advanced (LTE-Advanced) and Wireless Metropolitan Area Network Advanced (WirelessMAN-Advanced), both of which were technically specified in the 3rd Generation Partnership Project (3GPP) and in IEEE 802.16, respectively, are recognized as IMT-Advanced systems.

Existing conventional third-generation cellular systems aimed at providing wide coverage areas using macro base stations (abbreviated "Macro-BSs"). Deployment of Macro-BSs makes it possible for mobile user equipment (abbreviated "UE") to communicate anytime and anywhere through the wide coverage area provided by Macro-BSs. However, such a strategy of Macro-BS deployment is not sufficient to deal with the recent rapid increase in mobile data traffic. In addition, much mobile data traffic is generated in so-called hotspot areas, which are not geographically spread out.

In order to accommodate mobile data traffic in hotspot areas, a new concept called a "heterogeneous network (HetNet)" was proposed [4]–[6]. In a typical HetNet scenario, pico base stations (abbreviated "Pico-BSs"), with smaller transmission power and size than macro BSs, are deployed to efficiently accommodate mobile data traffic in hotspot areas within the coverage area of a Macro-BS. In short, Pico-BSs are overlaid on the Macro-BS coverage area. Another benefit of deploying Pico-BSs is to reduce coverage holes, where radio signal strength from Macro-BSs is so low that UEs are not served by Macro-BSs.

This paper is organized as follows. In Sect. 2, an overview of HetNet is presented. In order to simplify the analyses without loss of generality, this paper focuses on cases where Pico-BSs are overlaid on a Macro-BS coverage area using the same radio carrier frequency for the Pico- and Macro-BSs. This paper also shows the benefit from deployment of Pico-BSs, while pointing out drawbacks such as the limited amount of offloading of UEs from Macro-BSs to Pico-BSs and the occurrence of additional interference due to the deployment of Pico-BSs. Section 3 explains a technique called "cell range expansion (CRE)," which facilitates the offloading UEs from Macro-BSs to Pico-BSs, and then evaluates CRE for both full buffer and non-full buffer traffic models. In Sect. 4, a technique called "enhanced inter-cell interference coordination (eICIC)," which mitigates interference and increases system capacity [7], [8], is explained and evaluated. Section 5 presents uplink performance results rather than the downlink performance results in Sects. 3 and 4. Finally, Sect. 6 concludes the paper.

Manuscript received November 26, 2012.
Manuscript revised February 9, 2013.

[†]The author is with KDDI R&D Laboratories Inc., Fujiminoshi, 356-8502 Japan.
a) E-mail: skonishi@kddilabs.jp

DOI: 10.1587/transcom.E96.B.1243

2. Overview of Heterogeneous Networks (HetNet)

2.1 Concept of HetNet

The coverage areas in cellular systems are designed and constructed considering cost-effectiveness and available locations for BSs. In order to efficiently develop and expand coverage areas, Macro-BSs are firstly deployed in general. Once sufficient coverage area is established using Macro-BSs, the need for Macro-BSs will decrease, and not only Pico-BSs but also other wireless nodes, such as repeaters and Relays, will be suitable depending on the needs and considering their benefits such as small size, reasonable cost, and easy deployment [7]. An illustration of a HetNet with various wireless nodes is depicted in Fig. 1.

The wireless nodes that can be incorporated in the HetNet in Fig. 1 are briefly explained as follows.

2.1.1 Macro-BS

Macro-BSs are mainly used for wide coverage areas in a cellular network. The transmission power of Macro-BSs ranges from 10 to 40 W (or 40 to 46 dBm). The radius of the coverage area is from hundreds of meters to more than a few kilometers.

2.1.2 Pico-BS

Pico-BSs are used for not only coverage expansion to reduce coverage holes remaining after deployment of Macro-BSs but also for offloading mobile data traffic from Macro-BSs. Pico-BSs are sometimes regarded as Micro-BSs depending on the transmission power and the definition of terms. Their transmission power is from 1 to 8 W (or 30 to 39 dBm), and the radius of the coverage area is from tens to hundreds of meters.

2.1.3 Femto-BS

The transmission power of Femto-BSs is as small as that of UEs, for example 200 mW (or 23 dBm). A unique function of Femto-BSs is to utilize the access lines paid by customers such as optical fibers and asymmetric digital subscriber lines (ADSL) between homes and a local switch provided by a network operator, for instance.

Another noteworthy and unique idea for Femto-BSs is the closed subscriber group (CSG) [6]. When a CSG is adopted at a Femto-BS, no UEs can use the Femto-BS except the UEs registered at the Femto-BS. The CSG function may be used at homes and buildings for companies that want secured access to Femto-BSs. However, a CSG entails high interference for UEs that do not register at a Femto-BS, since such UEs cannot connect to the Femto-BS even when they are nearby, and then the UEs need to keep connecting with a Macro-BS using high transmission power [9], [10].

Their coverage area is narrower than Macro- and Pico-BSs, but Femto-BSs are easily deployed and cost effective.

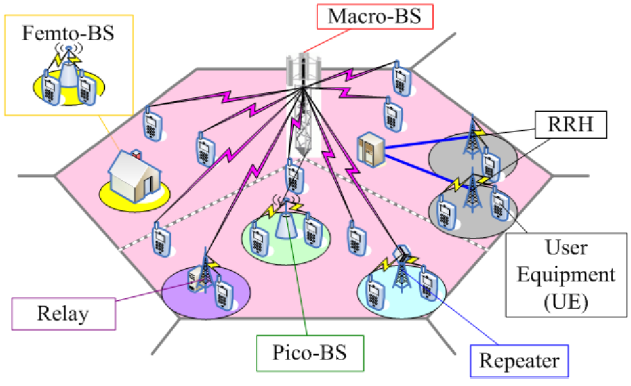

Fig. 1 Illustration of Heterogeneous Networks (HetNet) consisting of various kinds of wireless nodes.

2.1.4 Repeater

The main objective of repeaters is to expand the coverage area of BSs by retransmitting the radio signals received from the BSs. Repeaters can be deployed easily because repeaters do not require backhaul lines between the repeaters and core networks. Therefore, repeaters attract attention for their swift deployability, especially in emergencies and disasters. The transmission power of repeaters depends on the area to be covered but it varies from 250 mW (or 24 dBm) for small repeaters to 6 W (or 38 dBm) for large repeaters, in general.

2.1.5 Relay

A Relay is defined as one of the wireless nodes, where the signals transmitted from BSs are firstly decoded and then retransmitted as decoded signals to UE in the downlink, and vice versa in the uplink. The benefit of Relays is the improvement in the signal-to-interference-noise ratio (SINR) gained by omitting interference and noise at the Relays. This is different from Repeater, although Repeater and Relay have the common benefit that they do not need backhaul links. However, in Relays at least double transmission time is required from a BS to a UE and vice versa due to the decoding process at the Relays. In addition, several other functions, such as timing synchronization with the BS and the UE, as well as radio resource coordination between the link from the Relay to the UE and the link from the BSs to the Relay [11]. According to [12], the transmission power is assumed from 0.1 W (or 20 dBm) to 5 W (or 37 dBm) as for evaluation purposes.

2.1.6 Remote Radio Head (RRH)

RRHs unify antennas and circuits for both transmission and reception at radio frequency (RF). Since an RRH is connected to baseband units (BBU) at a BS through optical fibers, the RRH can easily expand the coverage area. The drawback of an RRH is the need for optical fibers between

RRH and BS. The transmission power of an RRH can be identical to that of various BSs such as the Macro-BS and Pico-BS. On the other hand, an RRH has an advantage over a Pico-BS from the viewpoint of easy adoption of functions requiring coordination and cooperation among multiple BSs, such as coordinated multiple transmission and reception points (CoMP), since all BBUs connected to RRHs and radio resource management functions for them are generally co-located [12].

2.2 Performance Improvement with Pico-BSs

As mentioned in Sect. 2.1, HetNet is composed of various wireless nodes. However, in order to simplify the investigation of the effectiveness of HetNet, this paper focuses only on a HetNet consisting of Macro- and Pico-BSs, but without loss of generality.

First, a performance improvement is presented in this section when the number of Pico-BSs increases over the Macro-BS coverage area. Note that the geographical coverage area served by one of the sector antennas at a BS is called a "cell." It is assumed that there are three sectors per Macro-BS in the performance evaluation. The coverage area in a sector of a Macro-BS is called a "macro cell area" here. The term "macro cell area" is used regardless of whether or not Pico-BSs exist over the Macro-BS coverage area. It is assumed that only one cell exists per Pico-BS because an omni antenna is used at a Pico-BS.

The numerical results in terms of the throughput in macro cell area, which is called "macro cell area throughput" are presented in Fig. 2. Note that the simulation conditions commonly used throughout this paper are summarized in Table 1. It is noted that the simulation parameters for Macro-BSs are in line with 3GPP evaluation methodologies. 3GPP Case 1 as in Table A.2.1.1-1 and Table A.2.1.1-2 Case-1 in [13] is employed except that the carrier frequency is 800 MHz in this paper. Regarding simulation studies for HetNet with Pico-BSs, this paper also follows the 3GPP evaluation methodologies in Table A.2.1.1.2-3 Model 1 for the path loss model and Table A.2.1.1.2-5 Configuration #4b for clustered UE distributions [13]. The simulation model based on Table A.2.1.1.2-5 Configuration #4b defines that 20 out of 30 UEs are equally distributed over the total number of Pico-BSs [13]. For instance, the number of UEs near one Pico-BS is 5 when the total number of Pico-BSs is 4 in a macro cell area. In the following simulation studies, the number of Pico-BSs is selected to be 1, 2, 4, 5, and 10 in the simulation study because 20 is divisible by those values.

Note that the full buffer model is used in this Sect. as a traffic model for the simulation study because the full buffer traffic model is useful to investigate the system capacity. Non-full buffer traffic model is also used from the following Sect. In addition, the numerical results presented up to Sect. 4 are only for the downlink, which is defined as the link from BSs to UEs. Sect. 5 provides numerical results for the uplink.

In Fig. 2, the macro cell area throughput, which is defined as the sum of user throughput of UEs, is presented. Note that "MUE" and "PUE" represent UEs served by a Macro-BS and a Pico-BS, respectively. In addition, "All UEs" refers to UEs on any BS type. Hence, the total number of All UEs is equal to the sum of the number of MUEs and PUEs. We observe that the throughput of PUEs increases as the number of Pico-BSs increases per Macro-BS because the SINR of UEs that change from MUEs to PUEs improves together with the deployment of Pico-BSs. This contributes to the increase of the macro cell area throughput representing "All UE" in the figure. On the other hand, the throughput of MUEs does not increase greatly even when the number of Pico-BSs increases. This is because cell-edge MUEs still exist even when the number of Pico-BSs increases, and therefore, the SINR distribution of MUEs does not change significantly. Since the full buffer traffic model is used, the sum of the UE throughput does not change much if the SINR distribution also does not change much.

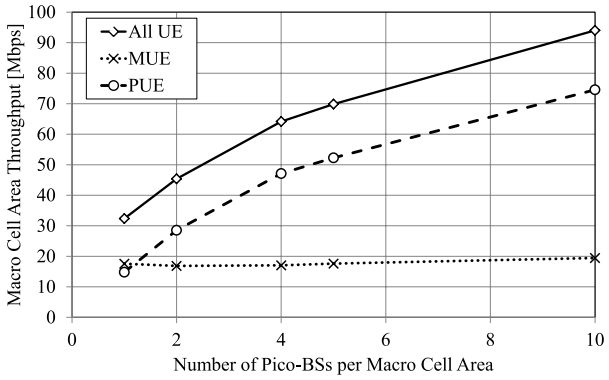

Fig. 2 Improvement of macro cell area throughput by deploying Pico-BSs over Macro-BS coverage area.

Table 1 Simulation parameters.

	Macro-BS	Pico-BS
Carrier frequency	800 MHz	
System bandwidth	10 MHz	
Cellular layout	7 tri-sectored hexagonal cells	1, 2, 4, 5, 10 Pico-BSs per sector of Macro-BS
Inter-Site distance	500 m	
Pathloss (d in km)	7.0 + 37.6 log10(d) dB	21.4 + 39.8 log10(d) dB
Shadowing standard deviation	10 dB	
Shadowing correlation	0.5 (between cells), 1.0 (between macro sectors in the identical cell)	
Fading model	SCM (urban macro with angular spread of 8 deg.)	
Penetration loss	20 dB	
Maximum Tx-power	46 dBm	30 dBm
Antenna height	32 m	18 m
Antenna gain with cable loss	14 dBi	5 dBi
Number of Tx-/Rx-antennas	2/2	
Antenna interval	10 λ	
MIMO scheme	Open-loop spatial multiplexing with rank adaptation	
UE receiver type	MMSE	
Noise figure	5 dB	
Moving speed	3 km / h	
Number of UEs	30 per sector	
UE drop	Clustered distribution (Config. #4b in [12])	
Scheduling algorithm	Proportional fair scheduling [14]	

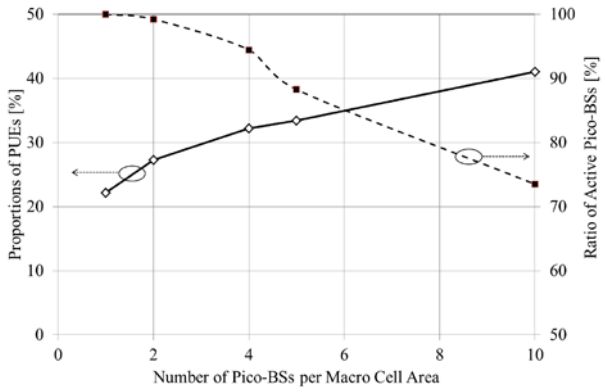

Fig. 3 Proportions of PUEs and active Pico-BSs when the number of Pico-BSs per macro cell area increase.

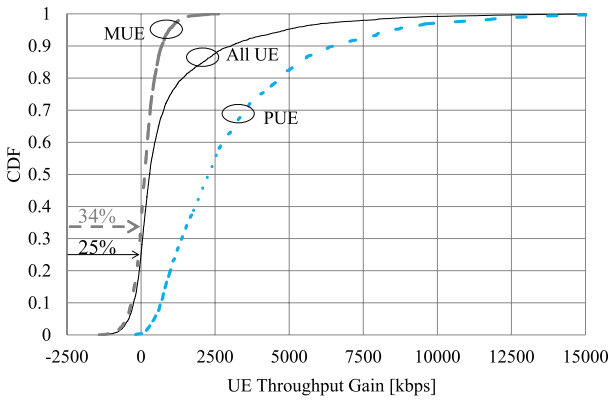

Fig. 4 CDF of UE throughput gain for cases with zero and two Pico-BSs.

The proportion of PUEs among all UEs is summarized in Fig. 3. In LTE system, the serving BS, which is the BS connected to a UE, is selected based on the reference signal received power (RSRP) in the downlink. Namely, the BS giving the maximum RSRP to a UE is selected as the "serving BS" for the UE. As the number of Pico-BSs increases, the proportion of PUEs increases. This trend is in line with the macro cell area throughput for the PUEs, as in Fig. 2. However, the proportion of PUEs does not increase as much. When we observe the proportion of active Pico-BSs (i.e. Pico-BSs serving at least one PUE) in Fig. 3, it is found that all the Pico-BSs are not in use, especially in cases with a large number of Pico-BSs. Although Pico-BSs are placed at hotspots according to the simulation model, there are Pico-BSs that serve no UEs. This comes from the simulation assumptions for the UE drop in Table 1. In the UE drop model, the total number of UEs in hotspots is fixed as 20, regardless of the number of Pico-BSs [13]. As the number of Pico-BSs per macro cell coverage area increases, the number of UEs per hotspot decreases. Due to the shadowing model in Table 1, all the UEs in a hotspot are not served by the center of the hotspot. This phenomenon occurs more in accordance with increase of the number of Pico-BSs per macro cell coverage area, since the Pico-BSs are closer to each other as the number of Pico-BSs is large. This investigation implies that we may end up wasting Pico-BSs. In this sense, we need a way to offload more MUEs to PUEs. Then, we can expect further improvement of macro cell area throughput with efficient use of all the Pico-BSs. Henceforth, this paper assumes two Pico-BSs per Macro-BS coverage area in the remaining of the paper, since both of two Pico-BSs will likely be active with more than 99% probability and the introduction of multiple Pico-BSs makes it possible to observe the mutual interference of multiple Pico-BSs in each macro cell coverage area in addition to the interference between Macro- and Pico-BSs.

Figure 4 gives numerical results showing whether or not UE throughput is improved after deploying two Pico-BSs. The throughput gain in the figure is defined as follows,

$$T_i^{\mathrm{HetNet}} - T_i^{\mathrm{HomoNet}}, \tag{1}$$

where T_i^{HetNet} and T_i^{HomoNet} are the throughput of UE i in a HetNet with two Pico-BSs in the macro cell coverage area and one in a homogeneous network with only Macro-BSs and without Pico-BSs. Most PUEs obtain positive throughput gain due to improvement in SINR and having sufficient radio resources available to PUEs from the deployment of Pico-BSs, although the rest of the PUEs suffer from increased interference from Macro-BSs. However, the throughput gains in approximately 34% of MUEs are negative. In other words, 34% of MUEs lose throughput after the deployment of two Pico-BSs. Overall, as we see from the cumulative distribution function (CDF) curve for "All UE" in the figure, approximately 75% of all UEs are able to obtain higher throughput after the introduction of Pico-BSs.

The fact that all the UEs cannot improve their throughput is one of the issues with HetNet. A solution to deal with this issue is discussed in Sect. 4.

3. Cell Range Expansion (CRE)

3.1 Concept of CRE

Section 2.2 reveals that it is better to increase the PUE ratio for the purpose of improving macro cell area throughput. For the purpose of further offloading UEs from MUEs to PUEs, a new technique named CRE was proposed [7], [8]. In this subsection, CRE is explained, then performance evaluation results are presented.

Figure 5 illustrates the concept of CRE. CRE connects UEs to Pico-BSs rather than Macro-BSs by adding a bias value called the "CRE bias value" to the signal level received from Pico-BS transmissions, when UEs select the serving BS that provides the greatest reference signal strength. Let RSRP from BS n and the CRE bias value for the BS be denoted by P_n [dB] and B_n [dB], respectively, for the UE. Then, the UE selects the serving BS that connects with the UE by the following equation,

$$\arg\max_n \{P_n + B_n\}. \tag{2}$$

For the purpose of CRE for Pico-BSs, B_n is selected to be a positive value for Pico-BSs while B_n is fixed at zero

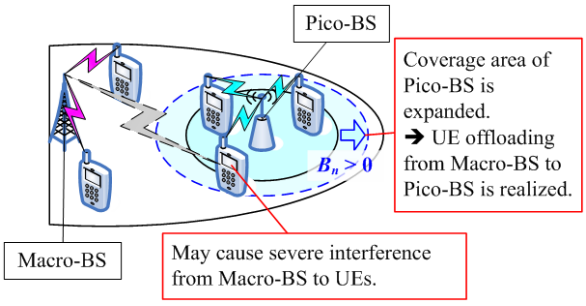

Fig. 5 Coverage area expansion of Pico-BSs by Cell Range Expansion (CRE).

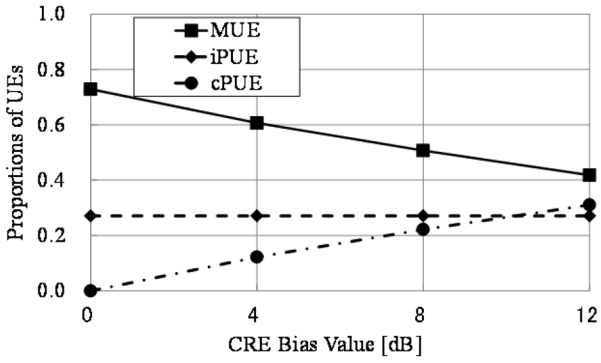

Fig. 6 UE ratios vs. CRE bias values to see offloading effect by CRE.

for Macro-BSs, in general. Note that the CRE bias value does not virtually enlarge the transmission power from Pico-BSs but makes UEs do handovers earlier to the BSs with a positive CRE bias value [15].

If the serving BS becomes a Pico-BS for a UE due to the CRE bias value, then the UE is offloaded from a Macro-BS to the Pico-BS. Such a UE connected to a Pico-BS due to CRE is called "cPUE," hereafter. On the other hand, a UE inherently connected to a Pico-BS even without CRE is called "iPUE" hereafter. Let sets of iPUEs and cPUEs be denoted by S_{iPUE} and S_{cPUE}. Then we can define a set of PUEs labeled S_{PUE}, thus:

$$S_{\mathrm{PUE}} = S_{\mathrm{iPUE}} \cup S_{\mathrm{cPUE}}. \tag{3}$$

The proportions of MUEs, iPUEs, and cPUEs are presented in Fig. 6 as the CRE bias value increases when the number of Pico-BSs is two per macro cell area. It is also assumed that the CRE bias value is identical for all Pico-BSs. As observed in the figure, the proportion of cPUEs increases as the CRE bias value increases. This means that the total number of UEs served by Pico-BSs increases, since the proportion of iPUEs is constant regardless of the CRE bias values. Contrary to the increase in PUEs, the proportion of MUEs decreases. For instance, when the CRE bias value is selected as 8 dB, almost half of UEs are offloaded from Macro-BSs to Pico-BSs, because the proportion of MUEs is roughly 50% according to the results in Fig. 6.

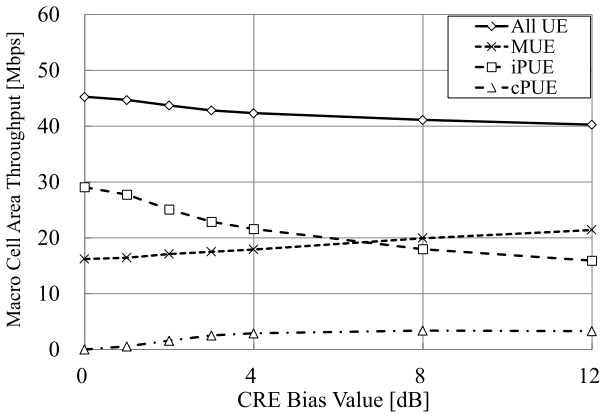

Fig. 7 Macro cell area throughput for All UEs as well as that for UEs served by Macro-BSs (MUE), UEs inherently served by Pico-BSs without CRE (iPUE), and UEs served by Pico-BSs due to CRE (cPUE) when the CRE bias value changes.

3.2 Performance Evaluations of CRE

3.2.1 Full Buffer Traffic Model

In this subsection, this paper presents the throughput changes resulting from the absence of CRE. In order to keep the identical simulation conditions with previous numerical results, the full-buffer model is used at first.

Figure 7 shows macro cell area throughput for all UEs, which is represented by "All UE" in the figure, as well as macro cell area throughput values for the various UE types such as MUE, iPUE, and cPUE, when the CRE bias value changes. Note that the sum of the macro cell area throughputs of MUEs, iPUEs, and cPUEs is equal to the macro cell area throughput for All UEs.

As we observe from the figure, the macro cell area throughput for All UEs decreases as the CRE bias value increases. This comes from the decrease of the macro cell area throughput of iPUEs, although those for MUEs and cPUEs increases as the CRE bias value increases. The reason why the macro area throughput of iPUEs decreases is that the total frequency resources of a Pico-BS are shared among not only iPUEs but also the cPUEs that are newly connected to the Pico-BS due to CRE. Since the SINR values of cPUEs are worse than iPUEs, the overall spectral efficiency in the Pico-BS degrades as the number of cPUEs increases. It is noteworthy that the coverage area of a Pico-BS tends to be larger as the location of the Pico-BS is farther from the Macro-BS associated with the Pico-BS [16]. This means that the MUEs in the cell edge of the macro cell coverage area tend to become cPUEs, whose SINR values tend to be low. Thus, the SINR values of MUEs tend to become higher, and then the spectral efficiency in Macro-BS becomes higher as a result.

Similar to Fig. 4, the throughput gain for every UE is presented in Fig. 8 when CRE is applied. Note that the CRE bias value is 8 dB. The figure shows that the fairness among

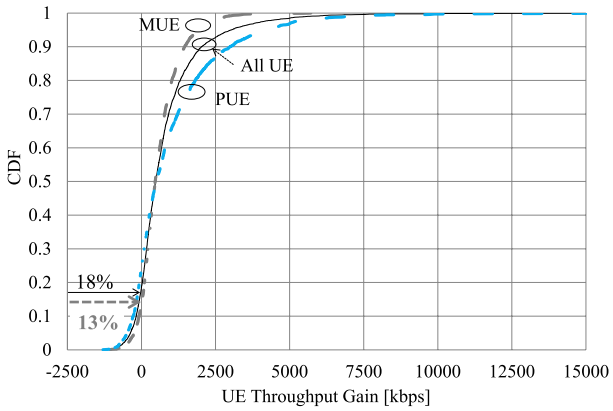

Fig. 8 CDF of UE throughput gain without Pico-BSs versus that with two Pico-BSs per macro cell area when the CRE bias value is 8 dB.

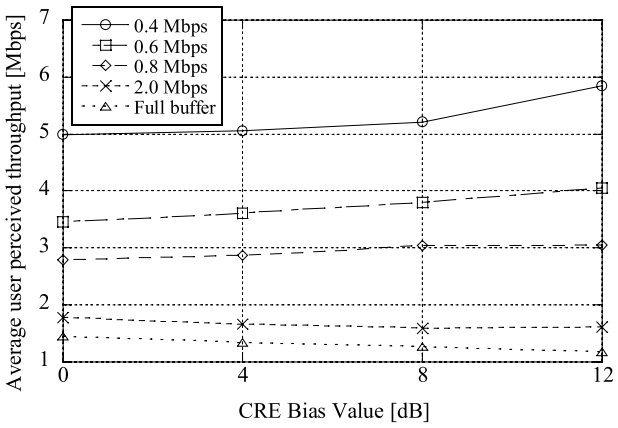

Fig. 9 Average user-perceived throughput (UPT) for various traffic models including the non-full buffer traffic model when the CRE bias value changes.

UEs is improved by having CRE rather than not, since all three CDF curves are close each other. In addition, the proportion of All UEs with negative throughput gain decreases from 25% to 18%. The ratio of MUEs with negative throughput gain decreases from 34% to 13%, due to the improvement in SINR values as explained in the previous paragraph.

3.2.2 Non-full Buffer Traffic Model

In addition to the full buffer traffic model presented in the previous subsection, a non-full buffer traffic model is also used to validate the CRE scheme. It gives a more complete picture to observe how the CRE scheme affects throughput in the non-full buffer traffic model, because it causes less interference than the full-buffer traffic model. The non-full buffer traffic model used in the simulation study follows the file transfer protocol (FTP) model described in [17]. The average, standard deviation, and maximum of Internet Protocol (IP) packet size are fixed at 10, 4, 25 kbytes, respectively. The amount of traffic generated (called "offered traffic," hereafter) per UE is configured by changing the average value of the arrival interval of IP packets. The offered load used for the simulation study is from 0.4 to 2.0 Mbps per UE. Since there are 30 UEs per macro cell area, the total offered traffic is up to 60 Mbps. This implies that the non-full buffer traffic model with such a high offered traffic behaves similarly to the full buffer traffic model because 60 Mbps is beyond the maximum value of the macro cell area throughput, as in Fig. 7.

Figure 9 shows the throughput performances when the CRE bias value changes. Since a non-full buffer traffic model is used, a metric named "user-perceived throughput (UPT)" is applied [12]. The UPT is defined as the total number of bits successfully transmitted for the UE divided by the length of time when data is queued at the transmission buffer for the UE. We can regard UPT as the instantaneous throughput when a UE has data to transmit or receive. Note that the difference from the "throughput" for the full buffer traffic model is the denominator in the throughput calculation. The denominator is the entire length of the simulation time for the full buffer traffic model. It is also noted, however, that when the full buffer traffic model is used, the UPT is equal to the throughput value in the case of the full buffer traffic model, since the transmission buffer is filled with data for every UE.

As we observe in Fig. 9, the average UPT is inversely proportional to the offered traffic per UE. As the offered traffic per UE decreases, the UPT increases. When the offered traffic is small, the radio resources required to transmit the offered traffic per UE decrease. This means sufficient radio resources are available to transmit the small amount of offered traffic per UE. In such a situation, it is easy to instantaneously transmit that small amount of traffic using the adequate radio resources available for UEs. Therefore, a small offered traffic volume yields a high UPT.

The other trends we observe from the figure are that the average UPT increases as the CRE bias value increases for low offered traffic, while the opposite trend is observed for high offered traffic. In the case of low offered traffic, the interference level from Macro-BSs to PUEs, especially to cPUEs, is small. In such a situation, the SINR of cPUEs does not become very low. Since many MUEs with low SINR become cPUEs when CRE bias values are large, the average SINR value of the remaining MUEs becomes higher than with small CRE bias values. In addition, the available radio resources per MUE increase, since the proportion of MUEs decreases as in Fig. 6. Therefore, MUEs can increase their UPT. On the other hand, when the offered traffic is high, the interference level from Macro-BSs to cPUEs becomes high. Then, both the SINR values and available radio resources for both cPUEs and MUEs decrease. Hence, UPT decreases when the CRE bias value increases. These phenomena are similar to the observations about the full-buffer traffic model using Fig. 7.

In conclusion, CRE is effective not only to facilitate offloading UEs from Macro-BSs to Pico-BSs but also to improve fairness among All UEs. In addition, CRE can enhance UPT, especially when offered traffic or radio resource

usage is small.

4. Enhanced Inter-Cell Interference Coordination (eICIC)

4.1 Concept of eICIC

CRE has several benefits, as introduced in Sect. 3.2. However, the greatest disadvantage of CRE is to decrease the macro cell area throughput, which corresponds to system capacity, according to the evaluation using the full buffer traffic model. The dominant factor behind CRE decreasing the system capacity is that it causes severe interference from Macro-BSs to cPUEs, especially when the CRE bias value is high. In order to mitigate this issue, we need an inter-cell interference coordination scheme. 3GPP came up with a new idea for inter-cell interference coordination named eICIC (e.g. [6]). There are two ways to realize inter-cell interference coordination by utilizing radio resources orthogonally: one is based on the time domain, while the other way is based on the frequency domain [20], [21]. However, 3GPP focused only on how to mitigate interference when a single frequency carrier is available in a HetNet [23]. Hence, this paper will investigate only a time domain eICIC (in short, "eICIC," hereafter) as defined by 3GPP [23].

Figure 10 illustrates eICIC. In LTE, the duration of a subframe is defined as 1 ms, and radio resources are controlled and managed at every subframe. In eICIC, a part of subframes is used for inter-cell interference mitigation. As in Fig. 10, in addition to the LTE subframes, which will henceforth be called "normal subframes," hereafter in this paper, 3GPP defines another subframe, which is called "Almost Blank Subframes (ABS)" since most of the radio resources in ABSs are not used to transmit anything except the signals that are indispensable for LTE operation such as the Common Reference Signals (CRS) [19]. The number of CRSs transmitted from Macro-BSs depends on the kind of ABS. One is the "Multimedia Broadcast multicast service Single Frequency Network (MBSFN) ABS." MBSFN is prepared for Multimedia Broadcast and Multicast Service (MBMS) in LTE. MBSFN ABS does not have CRSs in the physical downlink shared data transmission channels (PDSCH), where data traffic is carried. The other one is Non-MBSFN ABS, which is made from the normal subframes and therefore, it has CRSs in PDSCH as illustrated in Fig. 11. In general, the interference level from Macro-BSs at ABSs is weaker than that at normal subframes.

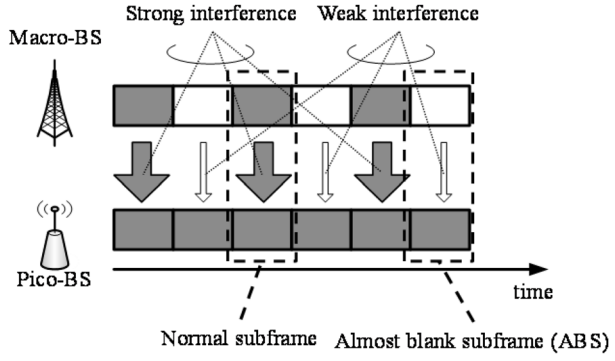

Fig. 10 Enhanced Inter-cell Interference Coordination (eICIC) for HetNet.

4.2 Performance Evaluation of eICIC

4.2.1 Full Buffer Traffic Model

Figure 12 shows the macro cell area throughput when eICIC is applied for various CRE bias values. The traffic model is the full buffer model. Note that we assume there are no CRSs in PDSCHs as there are MBSFNs in the ABSs in the following simulation studies of eICIC. Here, the "ABS ratio" on the horizontal axis in the figure is defined as the total duration of the ABSs out of 8 ms. The number of ABSs is selected from zero to seven out of eight subframes. When the ABS ratio is equal to zero, it means that eICIC is not applied. As we observe Fig. 12, eICIC seems more effective as the ABS ratio increases regardless of the CRE bias values.

In order to further investigate the details of macro cell area throughput, Fig. 13 is presented to show the macro cell area throughput for MUEs and PUEs as the ABS ratio increases. The relationship between the macro area throughput for All UEs, the macro area throughput for MUEs, and PUEs is expressed in the following equation.

$$\sum_{i \in S_{\text{AllUE}}} T_i = \sum_{j \in S_{\text{MUE}}} T_j + \sum_{k \in S_{\text{PUE}}} T_k, \tag{4}$$

where T_i, T_j, and T_k represent the UE throughput for All UE, MUE, and PUE, respectively. Similar to the notation

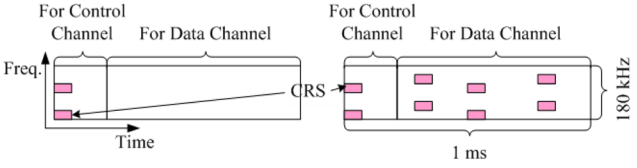

Fig. 11 Illustration of MBSFN ABS (left) and Non-MBSFN ABS (right).

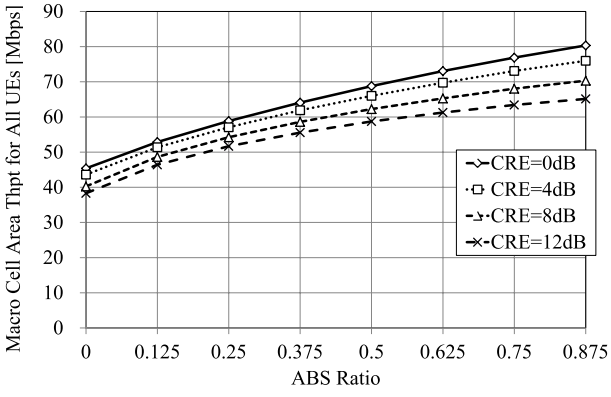

Fig. 12 Macro cell area throughput in downlink for various CRE bias values when the ratio ABSs changes.

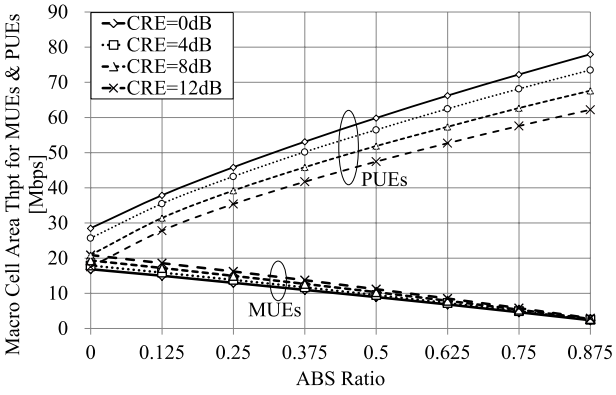

Fig. 13 Detailed numerical results for Fig. 12: Macro cell area throughput for MUEs and PUEs.

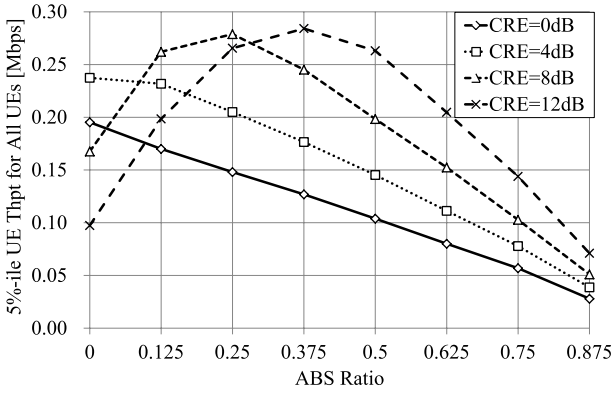

Fig. 14 5th percentile UE throughput among All UEs in downlink for various CRE bias values when the proportion of ABSs changes.

for S_{PUE} in Eq. (3), let S_{AllUE} and S_{MUE} be defined as the set of All UEs and MUEs, respectively. Note that the first term in the right hand side of the above equation is macro cell area throughput of MUEs. On the other hand, the second term represents the sum of the pico cell throughput values of two Pico-BSs per macro cell area.

As shown in Fig. 13, the cell throughput of PUEs increases due to the use of ABSs that provide SINR values improved for PUEs, although the macro cell area throughput of MUEs decreases because Macro-BSs cannot transmit data in the ABSs.

Note that the macro cell area throughput for MUEs increases as the CRE bias value increases. Contrary to this, the macro cell area throughput for PUEs decreases as the CRE bias value increases. Due to the fact that PUEs dominantly contribute to the value of the macro cell area throughput for All UEs, the highest macro cell area throughput is obtained when the CRE bias value is equal to zero, similar to the outcome demonstrated in Fig. 7.

Figure 14 shows the throughput value for the 5th percentile (5%-ile in the figure) UE in the CDF of UE throughput. In this case, the 5th percentile value among those for All UEs is presented for every CRE bias value and ABS ratio. Convex curves are observed in the figure. Figure 15,

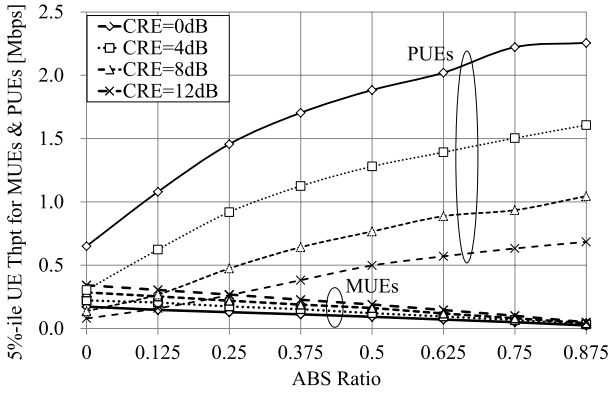

Fig. 15 Detailed numerical results for Fig. 14: 5th percentile UE throughput among MUEs and PUEs.

which shows the 5th percentile UE throughput value among MUEs and that among PUEs, explains the reason for the convex curves in Fig. 14.

The 5th percentile value in Fig. 14 depends on whether it is MUE or PUE that becomes the representative value for All UEs. When we focus on the CRE bias value of 12 dB, for instance, it is found that the curve for MUEs crosses that for PUEs when the ABS ratio is 0.25 in Fig. 15. The 5th percentile value among PUEs is smaller than that among MUEs when the ABS ratio is smaller than 0.25. Contrary to this, the curve for MUEs falls below that for PUEs in the figure when the ABS ratio is larger than 0.25. We can predict the convex curve by picking up the 5th percentile values for PUEs below where the ABS ratio is 0.25 and those for MUEs above there. A similar explanation can be applied to the other CRE bias values in general. It is noted that, due to the fact that the 5th percentile value for All UEs in Fig. 14 is not identical to those for MUEs and PUEs in Fig. 15, the absolute value and the ABS ratio with the peak value in Fig. 14 are not equal to those from Fig. 15. However, the reason why we observe convex curves in Fig. 14 can be revealed in such an analysis.

4.2.2 Non-full buffer traffic model

In addition to the full buffer traffic model, the effectiveness of eICIC is investigated for the non-full buffer traffic model that was introduced in Sect. 3.2. The simulation condition for the following numerical results is to use 0.4 Mbps as the offered traffic load per UE. Figure 16 shows the average UPT for All UEs when the ABS ratio changes to each of the four different CRE bias values. The trends of the average UPT are opposite for MUEs and PUEs, as in Fig. 17.

Unlike in the full buffer traffic model, there is a minimum value in terms of the average UPT regardless of the CRE bias values, as seen in Fig. 16. The overall results in Fig. 16 come from the average UPT for both MUEs and PUEs and the UE ratios shown in Fig. 17 and Fig. 6, respectively. In other words, the relationships of the average UPT values for All UEs, MUEs, and PUEs are given by the following equation.

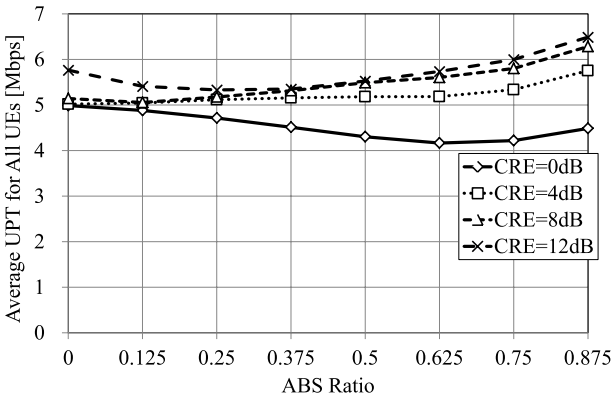

Fig. 16 Average UPT in downlink for various CRE bias values when the ratio of ABSs changes for an offered traffic load per UE of 0.4 Mbps.

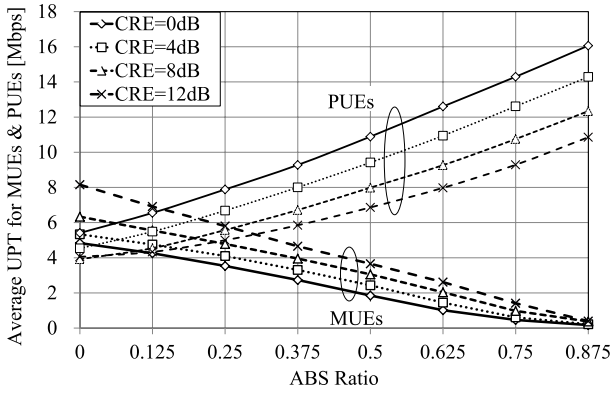

Fig. 17 Detailed numerical results for Fig. 16: Average UPT for MUEs and PUEs.

$$\mathrm{E}\{U_i\} = w_j \mathrm{E}\left\{U_j\right\} + w_k \mathrm{E}\{U_k\} \tag{5}$$

where E{x} is the mean value of the variable x. Note that U_i, U_j, and U_k represent the UPT for All UE, MUE, and PUE, respectively, in Eq. (5). The ratios of MUEs and PUEs are denoted w_j and w_k, respectively, and are found from the numerical results in Fig. 6.

Note that the trends in Fig. 17 show a similarity to Fig. 13 for the full buffer traffic model, although the trends in Fig. 16 are different from Fig. 12 for the full buffer traffic model. In addition, Fig. 16 shows that eICIC is effective for large CRE bias values under relatively low traffic loads with 0.4 Mbps as the offered traffic per UE. On the other hand, the opposite trend is found from Fig. 12 for the full-buffer traffic model that is the extreme case of a high traffic load.

With a high traffic load, the interference level from Macro-BSs to PUEs is high due to the use of a lot of radio resources for MUEs. Hence, large CRE bias values degrade the spectral efficiency of PUEs that suffer from high interference from Macro-BSs. Thus, small CRE bias values provide better performance with a high traffic load, as in Fig. 12. On the other hand, for relatively low traffic loads with 0.4 Mbps as the offered traffic per UE, the interference level from Macro-BSs to PUEs is low, as in the discussions regarding Fig. 9. Therefore, similar to the outcome from Fig. 9, the UPT becomes higher for higher CRE bias values, especially for MUEs as shown in Fig. 15. Note that as the ABS ratio in eICIC increases, radio resources with higher SINR values can be assigned to PUEs. Then, the UPT representing instantaneous throughput becomes high in eICIC. A high average UPT for PUEs in the case of small CRE values does not contribute to an increase in the overall average UPT shown in Fig. 16, since the ratio of PUEs is small when the CRE bias value is small.

It is noted here that 5th percentile UPT results show similar trends as the average UPT results, although numerical results are not presented in this paper due to limited space. Numerical results confirm that as the ABS ratio increases, the 5th percentile UPT for PUEs increases, while that for MUEs decreases.

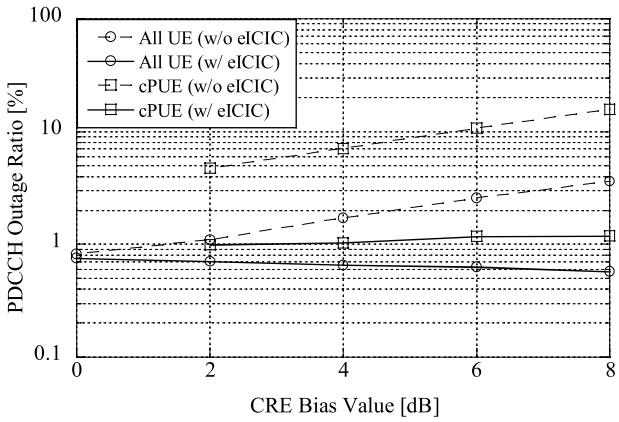

Fig. 18 Outage ratio of Physical Downlink Control CHannel (PDCCH) when an ABS ratio of 12.5% is used for eICIC.

4.2.3 Outage Ratio of Control Channel

The other benefit of using eICIC is here introduced. In LTE, there is a control channel called the "Physical Downlink Control Channel (PDCCH)," by which radio resource allocation information is transmitted to UEs before decoding the data channels named "Physical Downlink Shared Channel (PDSCH)" and "Physical Uplink Shared Channels (PUSCH)" for the downlink and uplink, respectively. UEs need to successfully decode PDCCH before data reception and transmission using PDSCH and PUSCH, respectively.

Figure 18 shows the PDCCH outage ratio, which is defined as the probability that the SINR becomes lower than the SINR value required to achieve 1% of the PDCCH packet error rate in this paper. Note that the ABS ratio is configured as 12.5% when eICIC is applied and the full buffer traffic model is used for evaluation.

It is found from the figure that the adaptation of CRE causes the PDCCH outage probability to exceed 1%. The main reason for this is that the PDCCH outage probability of cPUE reaches approximately 5% at the CRE bias value of 2 dB, for instance. However, we are able to decrease the PDCCH outage probability to around 1% even for cPUEs. For All UE, the PDCCH outage probability becomes less

than 1%. This comes from the fact that the PDCCH is transmitted to cPUEs in the ABSs with lower interference levels.

As demonstrated above, eICIC can also improve PDCCH performance.

5. Performance Evaluations for Uplink

In addition to the performance evaluations for the downlink provided in Sects. 3 and 4, this paper also presents numerical results for the uplink. In the simulation study of the uplink, this paper adopts the uplink transmission power control scheme specified in the LTE. The uplink transmission power $P(t)$ in decibel notation at time t is determined by the following equation [24].

$$P(t) = \min\{P_{\mathrm{CMAX}}, P_{\mathrm{O\_PUSCH}} + 10\log_{10}(M(t)) + \alpha \cdot PL + f(t)\}, \quad (6)$$

where P_{CMAX}, $M(t)$, PL, and $f(t)$ are the maximum transmission power available at a UE, the number of assigned resource blocks for the UE, the path loss value of the UE, and the compensation value for a closed-loop power control. Note that $P_{\mathrm{O\_PUSCH}}$ represents the target received signal power at the serving BS of the UE per resource block. When we increase $P_{\mathrm{O\_PUSCH}}$, a high received signal level is expected. However, this causes high interference in other UEs in the neighboring coverage area of adjacent BSs. In addition, when we select a large value for $P_{\mathrm{O\_PUSCH}}$, the transmission power of UE tends towards the upper limit P_{CMAX}. The path loss compensation factor α does not exceed 1.0. When α is equal to 1.0, the path loss is fully compensated regardless of UE location. In this case, the received power for cell-edge UEs becomes as high as that for cell-center UEs. However, this causes high interference in other UEs in neighboring BS's coverage areas. Reference [24] demonstrates that we are able to maximize UE throughput by adjusting the value of $P_{\mathrm{O\_PUSCH}}$. In this paper, both $P_{\mathrm{O\_PUSCH}}$ and α are selected as -80 dBm and 0.8, respectively, for the following evaluations. Note that the compensation value for closed-loop power control $f(t)$ is set to be zero.

As explained in Sect. 2.2, the BS with the maximum RSRP in the downlink is selected as the serving BS for both the downlink and uplink. Since the transmission power and antenna gain of Macro-BSs are higher than those of Pico-BSs as in Table 1, the coverage area of each Pico-BS becomes small. On the other hand, since the transmission power and antenna gain of a UE are identical regardless of the kinds of BSs from the viewpoint of the UE, it is the best for the uplink to select the BS with the minimum path loss value. In the uplink, unlike the downlink, it is found that CRE contributes to improvement of macro cell area throughput [24].

5.1 Full Buffer Traffic Model

This paper shows how eICIC affects the uplink performance when used in addition to CRE. Figure 19 shows the macro cell area throughput for All UEs in the case of the full buffer traffic model when both CRE and eICIC are applied similarly in the downlink. Figure 20 provides the details of macro cell area throughput for MUEs and PUEs.

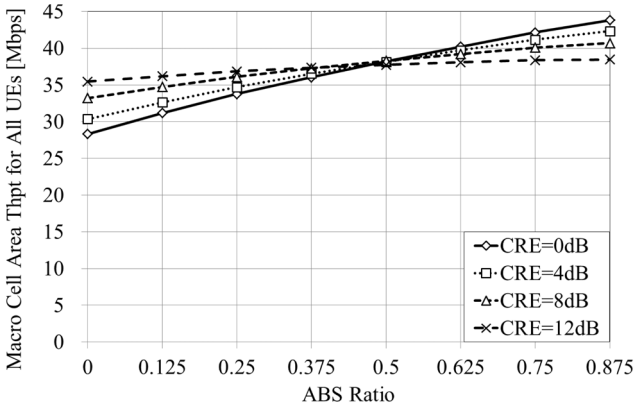

Fig. 19 Macro cell area throughput in uplink for various CRE bias values when the ratio of ABSs changes.

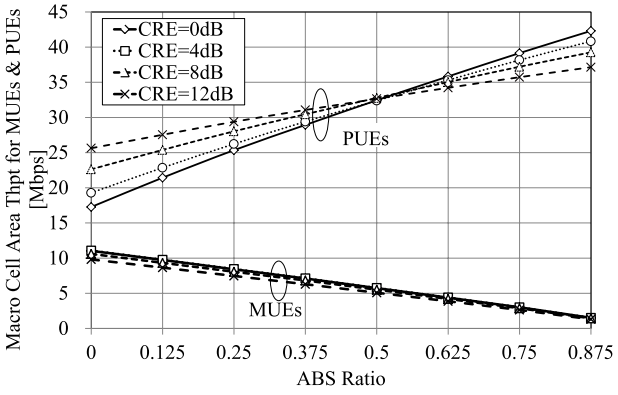

Fig. 20 Detailed numerical results for Fig. 19: Macro cell area throughput for MUEs and PUEs.

When the ABS ratio is equal to 0, meaning that eICIC is not applied, the macro cell area throughput increases as the CRE bias value increases as shown in Fig. 19. This is because a large CRE bias value compensates for the gap between the RSRP-based cell selection in the downlink and the path loss-based cell selection preferable for the uplink.

Next, we compare Fig. 12 and Fig. 19 for the downlink and uplink, respectively. It is found that the trends of numerical results in the uplink with an increase in ABS ratio are different from those in the downlink. When the ABS ratio is large enough to compensate for the path loss difference between Macro- and Pico-BSs, the SINR values of PUEs become high. Even in such a situation, the SINR values of iPUEs are higher than those of cPUEs in general because cPUEs suffer from higher interference from other BSs than iPUEs. In this situation, it is better to fully utilize radio resources for iPUEs with higher SINR rather than sharing the radio resources of Pico-BSs with cPUEs with lower SINR, to increase the macro cell area throughput. Hence, from the viewpoint of system capacity, small CRE bias values are

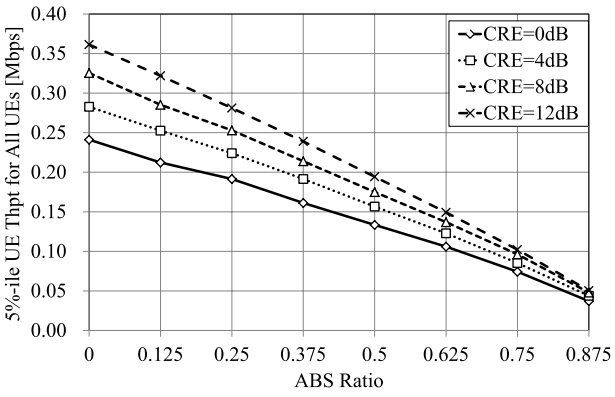

Fig. 21 5th percentile UE throughput among All UEs in uplink for various CRE bias values when the ratio of ABSs changes.

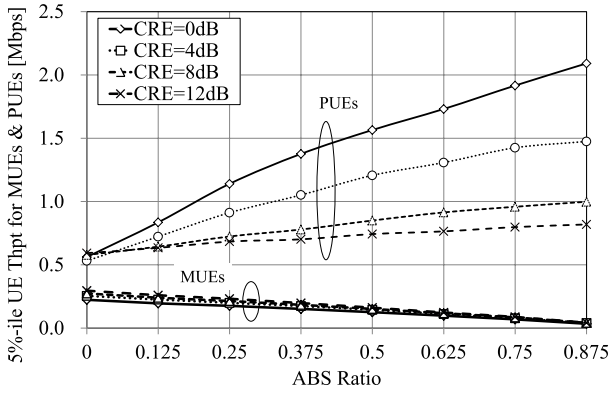

Fig. 22 Detailed numerical results for Fig. 21: 5th percentile UE throughput among MUEs and PUEs.

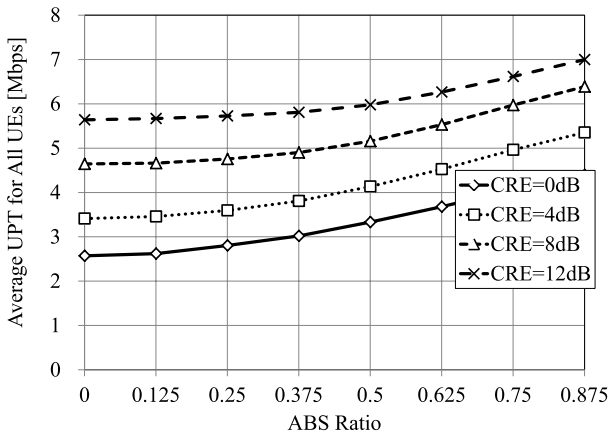

Fig. 23 Average UPT in uplink for various CRE bias values when the ratio of ABSs changes for the offered traffic load per UE is equal to 0.4 Mbps.

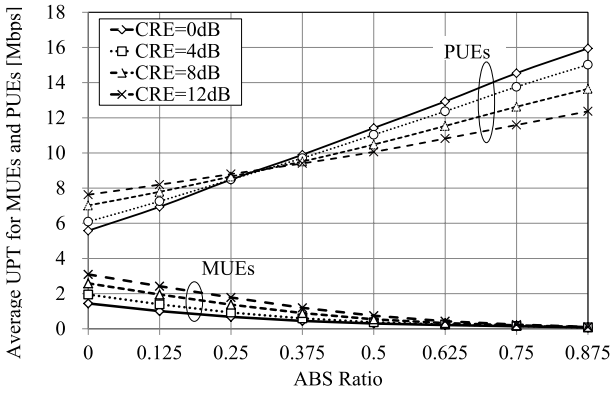

Fig. 24 Detailed numerical results for Fig. 23: Average UPT for MUEs and PUEs.

preferable, just as in downlink. On the other hand, when the ABS ratio is small, or when the ABS ratio is zero as the extreme case, PUEs including both iPUEs and cPUEs suffer from high interference caused by having MUEs located close to Pico-BSs. In such a case, CRE can mitigate interference from MUEs to PUEs because some MUEs become PUEs, and then they do not have to transmit unnecessary power to Macro-BSs. This utilizes the idea of path-loss based BS selection, which improves SINR values for UEs[†]. These considerations explain why the curves for small CRE bias values cross those for high CRE bias values as in Fig. 19 and the PUEs of Fig. 20.

The numerical results in terms of 5th percentile UE throughput for All UEs are presented in Fig. 21 and those for both MUEs and PUEs are summarized in Fig. 22. When we observe both the figures, we see that the 5th percentile UE throughput for All UEs comes from that of MUEs influenced by both the trends and their throughput values. From the viewpoint of MUEs, higher CRE bias values are preferable because more MUEs with low SINR become cPUEs, and then, the radio resources available in Macro-BSs are shared among remaining MUEs with relatively high SINR. Hence, higher CRE bias values are preferable from the viewpoint of 5th percentile UE throughput for All UEs.

5.2 Non-full Buffer Traffic Model

Figure 23 presents the average UPT for All UEs, while Fig. 24 shows those for MUEs and PUEs. It is clear that the trend of the average UPT for All UEs in Fig. 23 is different from that of the macro cell area throughput for All UEs in Fig. 19. The reason is explained in the following paragraphs.

Figure 20 demonstrates that the macro cell area throughput for MUEs in the uplink does not change greatly regardless of the CRE bias values, compared with the macro cell area throughput for PUEs. Since the macro cell area throughput for All UEs in Fig. 19 is from the summation of the macro cell area throughput for both MUEs and PUEs as described using Eq. (4), the trend of the macro cell area throughput for All UEs becomes similar to the one for PUEs in the case of full buffer traffic model.

On the other hand, the average UPT for All UEs is de-

[†]There is a method to further improve SINR values by selecting transmission power control parameters such as P_{O_PUSCH} and α [24]. However, due to space limitations this paper focuses on discussing the effectiveness of CRE and eICIC rather than transmission power control.

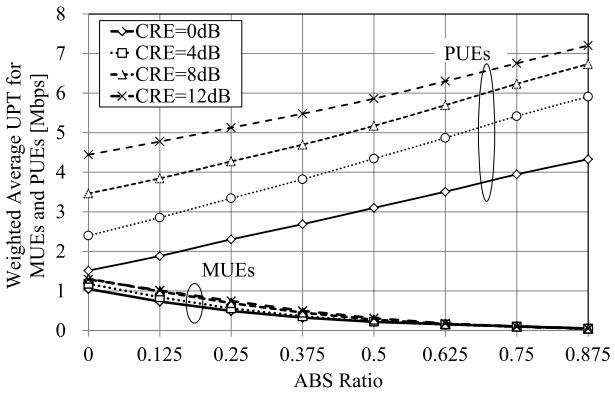

Fig. 25 Weighted average UPT for MUEs and PUEs corresponding to the first and second terms respectively in the right hand side of Eq. (5).

rived from Eq. (5), which is an equation with a weighted summation. As the CRE bias value increases, the ratio of PUEs increases, as explained using Fig. 3 in Sect. 2.2. Hence, the weighted average UPT values for PUE, corresponding to the second term on the right hand side of Eq. (5), become as shown in Fig. 25. According to Eq. (5), since the main contributor to the average UPT for All UEs is that of PUEs, the shape and trend in Fig. 23 resemble the weighted average UPT for PUEs in Fig. 25.

Due to space limitations, this paper does not show numerical results for 5th percentile UPT. From numerical results, in short, it is found that the trends are similar to those for the full buffer traffic models shown in Figs. 21 and 22. It is also confirmed that the values for MUEs determines that for All UEs.

6. Conclusions

This paper first introduced an overview of HetNet, which consists of various wireless nodes on top of Macro-BSs. Then, the effectiveness of deploying Pico-BSs over the macro cell coverage area, as well as its drawbacks was demonstrated by presenting numerical results. In order to overcome the drawbacks of Pico-BS deployment, this paper also showed not only how CRE affects throughput performance but also how eICIC works to mitigate inter-cell interference. In addition, this paper evaluated both the full buffer and non-full buffer traffic models as well as both the downlink and uplink, since they give different trends.

A comprehensive analysis of techniques such as CRE and eICIC showed the following:

- Deployment of Pico-BSs over the macro cell coverage area improves the macro cell area throughput due to the high SINR and sufficient radio resources available for PUEs. However, the drawback is that many MUEs suffer from additional interference caused by deployment of Pico-BSs, introducing unfairness between MUEs and PUEs.
- CRE works well for facilitating offload from MUEs to PUEs, although we need to bear some system capacity degradation in the downlink. However, unless the traffic load becomes high, CRE improves the user perceived throughput (UPT), which is a performance measure close to expressing the user experience for the non-full buffer traffic model. The unfairness between UEs incurred by Pico-BS deployment can be mitigated by CRE. In addition, CRE is useful for the uplink in LTE even with a high traffic load such as the full buffer traffic model, because CRE compensates for the gap of the serving BS selection, which is conducted based on RSRP in the downlink, although path-loss based selection is preferable from the viewpoint of uplink performance.
- The interference mitigation technique, eICIC, can increase the throughput of PUEs, although it decreases MUE throughput. It is also worth noting that eICIC can reduce the PDCCH outage probability.
- An MUE rather than a PUE becomes the 5th percentile UE among All UEs in the uplink regardless of the full and non-full buffer traffic models. This is because CRE is preferable in the uplink unless CRE bias value become so large. On the other hand, in the downlink, it depends on CRE bias values whether an MUE or a PUE becomes the 5th percentile UE among All UEs. In general, in the downlink, an MUE becomes the 5th percentile UE among All UEs for low CRE bias values, whereas a PUE becomes the 5th percentile UE among All UEs for high CRE bias values.

Due to space limitations, the author had to omit both evaluations of cases with more than two Pico-BSs per Macro-BS coverage area and discussions on handover performance in HetNet. As for the number of Pico-BSs, the performance trends presented in the paper will not change so much, according to the references [19], [20]. However, handover performance should be carefully investigated because of the negative effect of CRE on handover performance in various cell coverage areas of BSs. The author would like to rely on other papers for their discussion of this issue.

In addition, the selection of appropriate wireless nodes in HetNet is a challenging topic, as such a study requires a great deal of effort to investigate many combinations of wireless nodes.

Finally, the author would like to mention that studies on HetNet will be fundamental to studies aimed at further advanced technologies such as coordinated multiple points (CoMP) transmission and reception as well as small cell enhancements, both of which are regarded as part of HetNet. Needless to say, such topics will become important not only for studies but also for real network deployment.

Acknowledgments

The author would like to express appreciation to Messrs. N. Miyazaki of KDDI Corp. and M. Fushiki of KDDI R&D Laboratories Inc. for providing numerical results for this paper.

References

[1] http://www.soumu.go.jp/main_sosiki/kenkyu/global_ict/wireless_broadband.html
[2] Report ITU-R M.2243, "Assessment of the global mobile broadband deployments and forecasts for International Mobile Telecommunications," Nov. 2011.
[3] Recommendation ITU-R M.2012, "Detailed specifications of the terrestrial radio interfaces of International Mobile Telecommunications Advanced (IMT-Advanced)," Jan. 2012.
[4] R. Madan, J. Borran, A. Sampath, N. Bhushan, A. Khandekar, and T. Ji, "Cell association and interference coordination in heterogeneous LTE-A cellular networks," IEEE J. Sel. Areas Commun., vol.28, no.9, pp.1479–1489, Dec. 2010.
[5] S. Brueck, "Heterogeneous networks in LTE-advanced," Proc. 8th International Symposium on Wireless Communication Systems (ISWCS), pp.171–175, Nov. 2011.
[6] A. Damnjanovic, J. Montojo, W. Yongbin, T. Ji, T. Luo, M. Vajapeyam, Y. Taesang, O. Song, and D. Malladi, "A survey on 3GPP heterogeneous networks," IEEE Wireless Commun., vol.18, no.3, pp.10–21, June 2011.
[7] D. Lopez-Perez, I. Guvenc, G. de la Roche, M. Kountouris, T.Q.S. Quek, and J. Zhang, "Enhanced intercell interference coordination challenges in heterogeneous networks," IEEE Wireless Commun., vol.18, no.3, pp.22–30, June 2011.
[8] D. Lopez-Perez, X. Chu, and I. Guvenc, "On the expanded region of picocells in heterogeneous networks," IEEE J. Sel. Top. Signal Process., vol.6, no.3, pp.281–294, March 2012.
[9] A. Barbieri, A. Damnjanovic, T. Ji, J. Montojo, Y Wei, D. Malladi, O. Song, and G. Horn, "LTE femtocells: System design and performance analysis," IEEE J. Sel. Areas Commun., vol.30, no.3, pp.586–594, April 2012.
[10] N. Miyazaki, X. Wang, M. Fushiki, and S. Konishi, "Interference coordination of the downlink control channel under macro-femto deployment in long term evolution system," Proc. 8th International Symposium on Wireless Communication Systems (ISWCS), pp.332–336, Nov. 2011.
[11] S. Nagata, Y. Yan, A. Li, X. Gao, T. Abe, and T. Nakamura, "System performance investigation of layer-1 and layer-3 relays in LTE-Advanced downlink," IEICE Trans. Commun., vol.E94-B no.12, pp.3296–3303, Dec. 2011.
[12] D. Ogata, A. Nagate, and T. Fujii, "Multi-BS cooperative interference control for LTE systems," Proc. IEEE 75th Vehicular Technology Conference (VTC2012-Spring), May 2012.
[13] 3GPP TR36.814 v9.0.0, "Further advancements for E-UTRA physical layer aspects," March 2010.
[14] Juan Wen, "On the proportional fairness scheduling in wireless OFDM systems," Proc. Wireless Communications Networking and Mobile Computing (WiCOM) 2010, pp.1–4, Sept. 2010.
[15] K. Kitagawa, T. Komine, T. Yamamoto, and S. Konishi, "Performance evaluation of handover in LTE-Advanced systems with pico cell range expansion," Proc. 2012 IEEE 23rd International Symposium on Personal, Indoor and Mobile Radio Communications - (PIMRC), Sept. 2012.
[16] S. Landström, H. Murai, and A. Simonsson, "Deployment aspects of LTE pico nodes," Proc. Workshop on Heterogeneous Networks (HETnet) in 2011 IEEE International Conference on Communications (ICC), June 2011.
[17] NGMN, "Next generation mobile networks radio access performance evaluation methodology," Jan. 2008.
[18] M. Vajapeyam, A. Damnjanovic, J. Montojo, T. Ji, Y. Wei, and D. Malladi, "Downlink FTP performance of heterogeneous networks for LTE-advanced," Proc. Workshop on Heterogeneous Networks (HETnet) in 2011 IEEE International Conference on Communications (ICC), June 2011.
[19] N. Miki, Y. Saito, M. Shirakabe, A. Morimoto, and T. Abe, "Investigation on interference coordination employing almost blank subframes in heterogeneous networks for LTE-Advanced downlink," IEICE Trans. Commun., vol.E95-B, no.4, pp.1208–1217, April 2012.
[20] M. Shirakabe, A. Morimoto, and N. Miki, "Performance evaluation in heterogeneous networks employing time-domain inter-cell interference coordination and cell range expansion for LTE-Advanced downlink," IEICE Trans. Commun., vol.E95-B, no.4, pp.1218–1229, April 2012.
[21] N. Miki, A. Li, K. Takeda, Y. Yan, and H. Kayama, "Performance evaluation in heterogeneous networks employing time-domain inter-cell interference coordination and cell range expansion for LTE-Advanced downlink," IEICE Trans. Commun., vol.E94-B, no.12, pp.3312–3320, Dec. 2011.
[22] Y. Saito, J. Sangiamwong, N. Miki, S. Nagata, T. Abe, and Y. Okumura, "Performance evaluation in heterogeneous networks employing time-domain inter-cell interference coordination and cell range expansion for LTE-Advanced downlink," IEICE Trans. Commun., vol.E94-B, no.12, pp.3304–3311, Dec. 2011.
[23] 3GPP, RP-100383, "New work item proposal: Enhanced ICIC for non-CA based deployments of heterogeneous networks for LTE."
[24] A. Morimoto, N. Miki, H. Ishii, and D. Nishikawa, "Investigation on transmission power control in heterogeneous network employing cell range expansion for LTE-Advanced uplink," Proc. 18th European Wireless Conference, April 2012.

Satoshi Konishi received the B.S. and M.S. degrees in Electronic Engineering from the University of Electro-Communications (UEC), Tokyo, Japan, in 1991 and 1993, respectively. He also received the Ph.D. degree from Waseda University, Tokyo, Japan, in 2006. He joined Kokusai Denshin Denwa Co., Ltd., (now KDDI Corp.) in 1993. Since 1995, he has been engaged in research and development of radio resource allocation and management for wireless systems such as non-geostationary Earth orbit mobile satellite systems, fixed wireless access systems and cellular systems. He is the senior manager of Wireless Communications System Laboratory in KDDI R&D Laboratories Inc. His current research interests include the optimization of radio resources allocation, radio resource management, cross-layer control, multiple access techniques, adaptive transmission techniques and adaptive signal processing for mobile communications systems. Dr. Konishi received the Young Researchers' Award from IEICE and the "Meritorious Award on Radio" from the Association of Radio Industries and Businesses (ARIB) in 2000 and 2010, respectively. He is a member of IEEE.